

Signal Detection for OFDM and DS-CDMA with Gradient and Blind Source Separation Principles

M. G. S. Sriyananda, J. Joutsensalo, and T. Hämäläinen

Department of Mathematical Information Technology,

Faculty of Information Technology,

P.O. Box 35, FI-40014 University of Jyväskylä,

FINLAND

Email: {gamage.m.s.sriyananda, jyrki.j.joutsensalo, timo.t.hamalainen}@jyu.fi

Abstract : -Signal recovery mechanisms for both Orthogonal Frequency Division Multiplexing (OFDM) and Direct Sequence - Code Division Multiple Access (DS-CDMA) with the assistance of principles of Blind Source Separation (BSS) and Gradient Algorithms (GAs) are presented. Elimination or reduction of undesirable influences encountered with in the wireless interface is targeted using a set of filter coefficients. Four energy functions are used in deriving them. Time correlation properties of the channel are used as advantages in introducing the energy functions and they are tried to be justified followed by a performance evaluation. All the schemes are tested with synchronous downlink system models. Simulations are carried out under slow fading channel conditions with a receiver containing Equal Gain Combining (EGC) and BSS algorithms. It could be noted that, better performance for this predominant air interface communication techniques can be achieved with this combined schemes. It is important grasp the fact that, these schemes can be promoted as low complexity simple matrices based processing mechanisms.

Keywords — Blind Source Separation, Gradient Algorithms, OFDM, DS-CDMA, Slow Fading

1 Introduction

Distortion and mixing of signals during a process of air interface communication is a common scenario. About three main categories of signal recovery algorithms based on the availability of prior information about the mixing process or the mixture are found in statistical wireless signal processing. They are blind, semi-blind and non-blind or normal schemes. Two fundamental properties are emphasized by the adjective “blind”. First is no source signals are observed. Second is no information is available about the mixture. The implication of no prior information is available about the transfer is led by this. Therefore Blind Source or Signal Separation can be introduced as a process used for recovery of unobserved signals or sources from several observed mixtures. In implementations usually the observation values are obtained by output of a set of sensors. Sensors are designed such that each receives a different combination of the source signals. The core strength of the Blind Source Separation (BSS) model is the weakness or the least dependence on the prior information. That made it a versatile tool for extracting the spatial diversity provided by an array of sensors. A statistically strong plausible assumption of independence between the source signals is used to compensate the fact of lacking of prior knowledge about the mixture.

Outcomes of a attempt taken to derive a set of BSS schemes with the aid of gradient algorithm are disclosed in this paper and it is structured as follows. BSS solutions derived using the gradient principles are unveiled in Section 2. Then those solutions are converted to customized schemes for Orthogonal Frequency Division Multiplexing

(OFDM) and Direct Sequence - Code Division Multiple Access (DS-CDMA) systems. Two system models for baseband system simulations are discussed separately in Section 3. In Section 4, system parameters and simulation results are presented in detail. Finally conclusion is given in Section 5.

2 BSS Models and Gradient Algorithm

Having more sensors than sources in dealing with noisy observations, complex signals and mixtures are of much practical importance [1], [2]. Different types of approaches and solutions that take advantage of nonstationarity of sources to achieve better performance than the classical methods can be seen [3], [4]. Expansion and development of basic BSS models and algorithms in number of directions giving solutions for many complicated problems can be seen. They include noisy observations and complex signals and mixtures. Further they are applicable to the standard narrow band array processing or beamforming models and convolutive mixtures leading to multichannel blind deconvolution problems. Some of these approaches can only separate stationary non-Gaussian signals. Due to these limitations, poor performance is obtained when dealing with some real sources, like audio signals. Biomedical signal analysis and processing (ECG, EEG, MEG) [5], [6], [7] computer vision and image recognition, communications signal processing [8] are some of such most sensitive areas. Some disciplines that are not directly connected with the basic human needs,

economic or other profitable aspects like geophysical data processing, data mining, acoustics and speech recognition are being rapidly developed where a significant role can be played by Blind Source Separation (BSS) principles. Mathematical optimizations based on the principles of Gradient Algorithms (GAs) are widely used in the areas of civil, chemical, mechanical, and aerospace engineering, data networks, finance, supply chain management and many other areas [9].

It is shown that binary independent component analysis (ICA) can be uniquely identifiable under the disjunctive generation model [10]. Same time a deterministic iterative algorithm to determine the distribution of the latent random variables and the mixing matrix is proposed. These schemes can easily be applied for scenarios in network resource management. A generalization of the matched subspace filter for the detection of unknown signals in a background of non-Gaussian and nonindependent noise is unveiled in [11]. How efficiently the basic BSS theories can be applied in frequency domain is disclosed in [12]. In this approach, time-domain signals are transformed into time-frequency series and the separation is performed by applying ICA at each frequency envelope. It can be attempted to customize these approaches to any wireless communication system. A semi-blind compensation scheme for both frequency-dependent and frequency independent I/Q imbalance based on ICA in multiple-input multiple-output (MIMO) OFDM systems, where ICA is applied to compensate for I/Q imbalance and equalize the received signal jointly, without any spectral overhead is given in [13]. This can be recognized as an effort taken to improve the throughput performance of OFDM as same as the approach presented in this document.

2.1 General BSS Model

A number of successfully completed research studies targeting separation of sources on linear instantaneous mixtures can be found. They are with the vital primary assumption that the sources must be independent [3]. Here also a simple information symbol transfer process is considered. Source signals are denoted by $\mathbf{s}(t)$ with a mixture of coefficient values \mathbf{A} , where \mathbf{A} is a $F \times B$ matrix. Element f, b is denoted by $a_{f,b}$. $\mathbf{s}(t)$ is modeled with B signal elements as $\mathbf{s}(t) = [s_1(t), s_2(t), \dots, s_b(t), \dots, s_B(t)]^T$, where $s_b(t)$ is the signal element b at time t . Coefficient value of $s_1(t)$ is \mathbf{a}_1 , $\mathbf{a}_1 = [a_{1,1}, a_{2,1}, \dots, a_{f,1}, \dots, a_{F,1}]^T$. Additive independent and identically distributed (IID) white noise and colored noise are indicated by $\mathbf{w}(t) = [w_1(t), w_2(t), \dots, w_f(t), \dots, w_F(t)]^T$ and $\mathbf{w}'(t)$ respectively. $w_f(t)$ is the noise element f at time t . The receive signal matrix for a basic BSS process $\mathbf{x}(t) = [x_1(t), x_2(t), \dots, x_f(t), \dots, x_F(t)]^T$ at time t with B unknown input or sources and F output or sensor observations can be given as [3], [14] and [15],

$$\mathbf{x}(t) = \mathbf{A}\mathbf{s}(t) + \mathbf{w}(t) = s_1(t)\mathbf{a}_1 + \mathbf{w}'(t) \quad (1)$$

where $s_2(t), s_3(t), \dots, s_b(t), \dots, s_B(t)$ are independent or uncorrelated symbols or signals. Signal $s_1(t)$ is time correlated. When appropriately shaped mapped symbols are considered and the time delay is sufficiently shorter $c_1 = E\{s_1(t)s_1(t+\tau)\} \approx E\{s_1^2(t)\}$. The differential correlation matrix $\mathbf{C}(\tau)$ at a small time difference τ is given [16] as follows, where matrix transpose is symbolized by \cdot^T ,

$$\mathbf{C}(\tau) = E\{\mathbf{x}(t)\mathbf{x}^T(t+\tau)\} = c_1\mathbf{a}_1\mathbf{a}_1^T + \mathbf{R}_\tau \quad (2)$$

The ordinary correlation matrix \mathbf{R} is,

$$\begin{aligned} \mathbf{R} &= E\{\mathbf{x}(t)\mathbf{x}^T(t)\} \\ &= \mathbf{A}E\{\mathbf{s}(t)\mathbf{s}^T(t)\}\mathbf{A}^T + \sigma^2\mathbf{I} \\ &= c_1\mathbf{a}_1\mathbf{a}_1^T + \mathbf{R}_0 \end{aligned} \quad (3)$$

Noise variance is given by σ^2 . It is assumed that $\|\mathbf{R}_0\| > \|\mathbf{R}_\tau\|$, where $\|\cdot\|$ is Frobenius or 2-norm.

The output $\mathbf{y}(t)$ or \mathbf{y} of the receiver with coefficient \mathbf{u}_{rc} is,

$$\mathbf{y} = \mathbf{u}_{rc}^T \mathbf{x} \quad (4)$$

The output power $E\{\mathbf{y}^2(t)\}$ is derived by (3) and (4) as,

$$E\{\mathbf{y}^2(t)\} = \mathbf{u}_{rc}^T \mathbf{R} \mathbf{u}_{rc} \quad (5)$$

The energy functions $J_1(\mathbf{u}, \lambda_1)$, $J_2(\mathbf{u}, \lambda_2)$, $J_3(\mathbf{u}, \lambda_3)$ and $J_4(\mathbf{u}, \lambda_4)$ that are dependent of the measured signal values $\mathbf{x}(t)$ or \mathbf{x} are given in (6), (7), (8) and (9). \mathbf{u} is a variable coefficient similar to \mathbf{u}_{rc} . The differential cross correlation matrix \mathbf{C} is estimated same as the equation (2). $\lambda_1, \lambda_2, \lambda_3$ and λ_4 are the Lagrangian multipliers. Matrix inverse is referred by \cdot^{-1} .

$$J_1(\mathbf{u}, \lambda_1) = \mathbf{u}^T \mathbf{C} \mathbf{u} + \lambda_1 (\mathbf{I} - \mathbf{u}^T \mathbf{R} \mathbf{u}) \quad (6)$$

$$J_2(\mathbf{u}, \lambda_2) = \mathbf{u}^T \mathbf{C}^{-1} \mathbf{u} + \lambda_2 (\mathbf{I} - \mathbf{u}^T \mathbf{R} \mathbf{u}) \quad (7)$$

$$J_3(\mathbf{u}, \lambda_3) = \mathbf{u}^T \mathbf{C} \mathbf{u} + \lambda_3 (\mathbf{I} - \mathbf{u}^T \mathbf{R}^{-1} \mathbf{u}) \quad (8)$$

$$J_4(\mathbf{u}, \lambda_4) = \mathbf{u}^T \mathbf{C}^{-1} \mathbf{u} + \lambda_4 (\mathbf{I} - \mathbf{u}^T \mathbf{R}^{-1} \mathbf{u}) \quad (9)$$

The signal $s_1(t)\mathbf{a}_1$ is targeted to be extracted. In each of the (6) and (8), noise component of $\mathbf{w}'(t)$ is tried to be removed while passing the signal $s_1(t)\mathbf{a}_1$. In (7) or (9), it is the interference component in $\mathbf{w}'(t)$. In (6) or (8), the projection of \mathbf{u} to the effective space spanned by the matrix \mathbf{C} is tried to be minimized by the first terms. The output power to the inverse process is minimized by \mathbf{u} respectively where \mathbf{C} is produced. In all (6) - (9), time correlated signal portion $s_1(t)\mathbf{a}_1$ is included with \mathbf{C} . Resulting $\mathbf{u}^T \mathbf{C} \mathbf{u}$ is expected to be in minimum. It is expected that the signal $s_1(t)\mathbf{a}_1$ is passed quite well by \mathbf{u} . Minimization of the projection of \mathbf{u} to the effective spaces spanned by \mathbf{R} are tried by the second terms of the equations. Similarly minimization of the projection of \mathbf{u} to the effective space spanned by \mathbf{C}^{-1} is tried by the first terms of the (7) or (9). Here also the output power to inverse method is minimized by \mathbf{u} , with \mathbf{C}^{-1} is produced. Due to the inverse matrix, resulting $\mathbf{u}^T \mathbf{C}^{-1} \mathbf{u}$ is kept in minimum. It is expected to pass the signal $s_1(t)\mathbf{a}_1$ quite well by \mathbf{u} . Minimization of the projections of \mathbf{u} to the

effective spaces spanned by \mathbf{R}^{-1} are tried by the second terms of the equations. In all (6) - (9), $E\{\mathbf{y}^2(t)\}$ is tried to be minimized. But with correlation, \mathbf{R}_0 contains much the interference part of \mathbf{R} . In this case also the desired signal $s_1(t)\mathbf{a}_1$ is filtered well again by \mathbf{u} in the respective energy functions.

In the process of optimization, considering the partial derivatives $\frac{\partial J_1(\mathbf{u}, \lambda_1)}{\partial \lambda_1} = 0$ of (6), $\frac{\partial J_2(\mathbf{u}, \lambda_2)}{\partial \lambda_2} = 0$ of (7), $\frac{\partial J_3(\mathbf{u}, \lambda_3)}{\partial \lambda_3} = 0$ of (8) and $\frac{\partial J_4(\mathbf{u}, \lambda_4)}{\partial \lambda_4} = 0$ of (9),

$$(\mathbf{I} - \mathbf{u}^T \mathbf{R} \mathbf{u}) = 0 \quad (10)$$

$$(\mathbf{I} - \mathbf{u}^T \mathbf{R} \mathbf{u}) = 0 \quad (11)$$

$$(\mathbf{I} - \mathbf{u}^T \mathbf{R}^{-1} \mathbf{u}) = 0 \quad (12)$$

$$(\mathbf{I} - \mathbf{u}^T \mathbf{R}^{-1} \mathbf{u}) = 0 \quad (13)$$

Since (10) and (11) are in the same form, one common term can be defined as (14). It is considered as $\mathbf{u} = \mathbf{u}_1$ and these parameters are not to be used in (6) or (7). Similarly (12) and (13) are in the same form and one common term can be defined as (15). It is considered as $\mathbf{u} = \mathbf{u}_2$ and these parameters are not to be used in (8) or (9).

$$(\mathbf{I} - \mathbf{u}_1^T \mathbf{R} \mathbf{u}_1) = 0 \quad (14)$$

$$(\mathbf{I} - \mathbf{u}_2^T \mathbf{R}^{-1} \mathbf{u}_2) = 0 \quad (15)$$

Where \mathbf{u}_1 and \mathbf{u}_2 at time t are $\mathbf{u}_1(t)$ and $\mathbf{u}_2(t)$ respectively. Using (14), $\mathbf{u}_1(t)$ is defined in two forms $\mathbf{u}_{1,1}(t)$ and $\mathbf{u}_{1,2}(t)$ as used in (16) and (18) correspondingly. $\mathbf{u}_{1,1}^0(t)$ and $\mathbf{u}_{1,2}^0(t)$ are defined based on them. Using (15), $\mathbf{u}_2(t)$ is defined in two forms as $\mathbf{u}_{2,1}(t)$ and $\mathbf{u}_{2,2}(t)$ as presented by (20) and (22). $\mathbf{u}_{2,1}^0(t)$ and $\mathbf{u}_{2,2}^0(t)$ are defined based on them. They are all with similar kinds of approaches as the gradient algorithm [9]. Parameters given by $\mu_{\beta, \gamma}$, $\beta = 1, 2$ and $\gamma = 1, 2$ can be introduced as the corresponding forgetting factors for them. It is clear that $\mathbf{u}_{1,1}(t)$, $\mathbf{u}_{1,2}(t)$ and their associated parameters are common for both (6) and (7) while $\mathbf{u}_{2,1}(t)$, $\mathbf{u}_{2,2}(t)$ and their related parameters are common for both (8) and (9). Matrix complex conjugate transpose is denoted by $*$.

• *Common Coefficient 1*

$$\mathbf{u}_{1,1}^0(t) = \mathbf{u}_{1,1}(t) + \mu_{1,1} \left(\mathbf{I} - \mathbf{R} \cdot \mathbf{u}_{1,1}(t) \mathbf{u}_{1,1}^*(t) \right) \mathbf{C} \mathbf{u}_{1,1}(t) \quad (16)$$

$$\mathbf{u}_{1,1}^1(t) = \frac{\mathbf{u}_{1,1}^0(t)}{\|\mathbf{u}_{1,1}^0(t)\|} \quad (17)$$

• *Common Coefficient 2*

$$\mathbf{u}_{1,2}^0(t) = \mathbf{u}_{1,2}(t) + \mu_{1,2} \left(\mathbf{I} - \mathbf{R} \cdot \mathbf{u}_{1,2}(t) \mathbf{u}_{1,2}^*(t) \right) (\mathbf{C} + \mathbf{C}^*) \mathbf{u}_{1,2}(t) \quad (18)$$

$$\mathbf{u}_{1,2}^1(t) = \frac{\mathbf{u}_{1,2}^0(t)}{\|\mathbf{u}_{1,2}^0(t)\|} \quad (19)$$

• *Common Coefficient 3*

$$\mathbf{u}_{2,1}^0(t) = \mathbf{u}_{2,1}(t) + \mu_{2,1} \left(\mathbf{I} - \mathbf{R}^{-1} \cdot \mathbf{u}_{2,1}(t) \mathbf{u}_{2,1}^*(t) \right) \mathbf{C} \mathbf{u}_{2,1}(t) \quad (20)$$

$$\mathbf{u}_{2,1}^1(t) = \frac{\mathbf{u}_{2,1}^0(t)}{\|\mathbf{u}_{2,1}^0(t)\|} \quad (21)$$

• *Common Coefficient 4*

$$\mathbf{u}_{2,2}^0(t) = \mathbf{u}_{2,2}(t) + \mu_{2,2} \left(\mathbf{I} - \mathbf{R}^{-1} \cdot \mathbf{u}_{2,2}(t) \mathbf{u}_{2,2}^*(t) \right) (\mathbf{C} + \mathbf{C}^*) \mathbf{u}_{2,2}(t) \quad (22)$$

$$\mathbf{u}_{2,2}^1(t) = \frac{\mathbf{u}_{2,2}^0(t)}{\|\mathbf{u}_{2,2}^0(t)\|} \quad (23)$$

For the iteration m of any of the solutions in (17), (19), (21) or (23),

$$\mathbf{u}_c^m(t) = \frac{\mathbf{u}_c^{m-1}(t)}{\|\mathbf{u}_c^{m-1}(t)\|} \quad (24)$$

where $\cdot_{1,1}$, $\cdot_{1,2}$, $\cdot_{2,1}$ or $\cdot_{2,2}$ is represented by \cdot_c .

2.2 Gradient Algorithm Based BSS for OFDM

Higher rate transmission capability, higher bandwidth efficiency and robustness to multipath fading (including tolerance to frequency-selective fading) and delays are some of the key factors that brought Orthogonal Frequency Division Multiplexing (OFDM) techniques to the forefront of the sphere of wireless communication. Here the involvement of BSS algorithms and GA based approaches in a process of symbol recognition at a basic OFDM receiver is tested.

Wireless communication system consisting a N sub-carrier (N -point inverse discrete Fourier transform (IDFT)/discrete Fourier transform (DFT)) OFDM [17], [18] transmitter and a receiver is considered. Frequency response of the channel state information (CSI) of subcarrier n during an OFDM symbol period t is signified by $H_n(t)$. Impulse response of the path l of the channel tap k of the multipath frequency-selective Rayleigh fading channel within the same duration is symbolized by $h_{k,l}(t)$. Each tap is modeled with L independent paths with exponentially decaying delay profiles.

$$H_n(t) = \sum_{k=0}^{N-1} \sum_{l=0}^{L-1} h_{k,l}(t) e^{-j \frac{2\pi k n t}{N}} \quad (25)$$

Transmit symbol and normalized additive white Gaussian noise (AWGN) of subcarrier n for the period t are represented by $d_n(t)$ and $v_n(t)$ respectively. σ is the standard deviation to the additive white Gaussian noise. Then the receive signal $r_n(t)$ on subcarrier n during t can be expressed as in (26).

$$r_n(t) = H_n(t) d_n(t) + \left(\frac{\sigma}{\sqrt{2}} v_n(t) \right) \quad (26)$$

Considering the characteristics of a slow fading channel it can be assumed that for a given symbol frame, path gain $H_n(t) = H_n$ and $h_{k,l}(t) = h_{k,l}$.

$$r_n(t) = H_n d_n(t) + \left(\frac{\sigma}{\sqrt{2}} v_n(t) \right) \quad (27)$$

The receive signal samples of subcarrier n at the time period containing the symbol $d_n(t)$ can be expressed as $r_n(t), r_n(t + \tau), \dots, r_n(t + (p-1)\tau), \dots, r_n(t + (P-1)\tau)$. Where the P receive signal samples are taken with small time shifts of τ within each information symbol duration. These samples are equivalent to $x_1(t), x_2(t), \dots, x_f(t), \dots, x_F(t)$ in (1). Similar to (27), when symbol sample of $d_n(t)$ and AWGN of sample p of $r_n(t)$ are indicated by $d_n(t + (p-1)\tau)$ and $v_n(t + (p-1)\tau)$ correspondingly, sample p of receive signal $r_n(t)$ is given as,

$$r_n(t + (p-1)\tau) = H_n d_n(t + (p-1)\tau) + \left(\frac{\sigma}{\sqrt{2}} v_n(t + (p-1)\tau) \right) \quad (28)$$

For any symbol sample on subcarrier n within a time duration of a transmit symbol $d_n(t)$, $d_n(t + (p-1)\tau) = d_n(t)$.

$$r_n(t + (p-1)\tau) = H_n d_n(t) + \left(\frac{\sigma}{\sqrt{2}} v_n(t + (p-1)\tau) \right) \quad (29)$$

$\mathbf{r}_n(t)$ and $\mathbf{r}_n(t + \tau)$ are $Q \times Q$ square matrices containing these samples as elements and $(P-1) = Q^2$.

$$\mathbf{r}_n(t) = \begin{bmatrix} r_n(t) & \dots & \dots \\ \vdots & \ddots & \vdots \\ \dots & \dots & r_n(t + (P-2)\tau) \end{bmatrix} \quad (30)$$

$$\mathbf{r}_n(t + \tau) = \begin{bmatrix} r_n(t + \tau) & \dots & \dots \\ \vdots & \ddots & \vdots \\ \dots & \dots & r_n(t + (P-1)\tau) \end{bmatrix} \quad (31)$$

The differential correlation matrix $\mathbf{C}_n(\tau)$ at a small time difference τ and ordinary correlation matrix \mathbf{R}_n for subcarrier n according to (2) and (3) are,

$$\mathbf{C}_n(\tau) = \mathbf{E} \{ \mathbf{r}_n(t) \mathbf{r}_n^*(t + \tau) \} \quad (32)$$

$$\mathbf{R}_n = \mathbf{E} \{ \mathbf{r}_n(t) \mathbf{r}_n^*(t) \} \quad (33)$$

As in (16), (18), (20) and (22), matrices $\mathbf{u}_{1,1,n}(t)$, $\mathbf{u}_{1,2,n}(t)$, $\mathbf{u}_{2,1,n}(t)$, $\mathbf{u}_{2,2,n}(t)$ and associated matrices $\mathbf{u}_{1,1,n}^0(t)$, $\mathbf{u}_{1,2,n}^0(t)$, $\mathbf{u}_{2,1,n}^0(t)$, $\mathbf{u}_{2,2,n}^0(t)$ of subcarrier n for the algorithms can be presented as follows. $\mathbf{u}_{1,1,n}^m(t)$, $\mathbf{u}_{1,2,n}^m(t)$, $\mathbf{u}_{2,1,n}^m(t)$, $\mathbf{u}_{2,2,n}^m(t)$ are the corresponding coefficient matrices for iterations.

- *Common Coefficient 1 for Subcarrier n*

$$\mathbf{u}_{1,1,n}^0(t) = \mathbf{u}_{1,1,n}(t) + \mu_{1,1} \left(\mathbf{I} - \mathbf{R}_n \cdot \mathbf{u}_{1,1,n}(t) \mathbf{u}_{1,1,n}^*(t) \right) \mathbf{C}_n \mathbf{u}_{1,1,n}(t) \quad (34)$$

$$\mathbf{u}_{1,1,n}^m(t) = \frac{\mathbf{u}_{1,1,n}^{m-1}(t)}{\| \mathbf{u}_{1,1,n}^{m-1}(t) \|} \quad (35)$$

- *Common Coefficient 2 for Subcarrier n*

$$\mathbf{u}_{1,2,n}^0(t) = \mathbf{u}_{1,2,n}(t) + \mu_{1,2} \left(\mathbf{I} - \mathbf{R}_n \cdot \mathbf{u}_{1,2,n}(t) \mathbf{u}_{1,2,n}^*(t) \right) \cdot (\mathbf{C}_n + \mathbf{C}_n^*) \mathbf{u}_{1,2,n}(t) \quad (36)$$

$$\mathbf{u}_{1,2,n}^m(t) = \frac{\mathbf{u}_{1,2,n}^{m-1}(t)}{\| \mathbf{u}_{1,2,n}^{m-1}(t) \|} \quad (37)$$

- *Common Coefficient 3 for Subcarrier n*

$$\mathbf{u}_{2,1,n}^0(t) = \mathbf{u}_{2,1,n}(t) + \mu_{2,1} \left(\mathbf{I} - \mathbf{R}_n^{-1} \cdot \mathbf{u}_{2,1,n}(t) \mathbf{u}_{2,1,n}^*(t) \right) \mathbf{C}_n \mathbf{u}_{2,1,n}(t) \quad (38)$$

$$\mathbf{u}_{2,1,n}^m(t) = \frac{\mathbf{u}_{2,1,n}^{m-1}(t)}{\| \mathbf{u}_{2,1,n}^{m-1}(t) \|} \quad (39)$$

- *Common Coefficient 4 for Subcarrier n*

$$\mathbf{u}_{2,2,n}^0(t) = \mathbf{u}_{2,2,n}(t) + \mu_{2,2} \left(\mathbf{I} - \mathbf{R}_n^{-1} \cdot \mathbf{u}_{2,2,n}(t) \mathbf{u}_{2,2,n}^*(t) \right) \cdot (\mathbf{C}_n + \mathbf{C}_n^*) \mathbf{u}_{2,2,n}(t) \quad (40)$$

$$\mathbf{u}_{2,2,n}^m(t) = \frac{\mathbf{u}_{2,2,n}^{m-1}(t)}{\| \mathbf{u}_{2,2,n}^{m-1}(t) \|} \quad (41)$$

For OFDM systems, coefficient matrix $\mathbf{u}_{c,n}^m(t)$ for the iteration m for subcarrier n of any of the solutions given by $\mathbf{u}_{1,1,n}^m(t)$, $\mathbf{u}_{1,2,n}^m(t)$, $\mathbf{u}_{2,1,n}^m(t)$ or $\mathbf{u}_{2,2,n}^m(t)$ is stated as in (42). But $\mathbf{u}_{c,n}^m(t)$ is different according to each scenario presented in (35), (37), (39) and (41).

$$\mathbf{u}_{c,n}^m(t) = \frac{\mathbf{u}_{c,n}^{m-1}(t)}{\| \mathbf{u}_{c,n}^{m-1}(t) \|} \quad (42)$$

Refined receive signal similar to (4) is,

$$\mathbf{y}'_n(t) = \mathbf{u}_{c,n}^{m*}(t) \mathbf{r}_n(t) \quad (43)$$

Elements of matrix $\mathbf{y}'_n(t)$ can be defined as $y'_n(t), y'_n(t + \tau), \dots, y'_n(t + (p-1)\tau), \dots, y'_n(t + (P-1)\tau)$ similar to (27). Signal after Equal Gain Combining (EGC) can be expressed as,

$$\mathbf{y}_n(t) = \frac{1}{Q^2} \frac{H_n^*}{|H_n|^2} \sum_{p=1}^P y'_n(t + (p-1)\tau) \quad (44)$$

The simplified matrix format of the receiver output $\mathbf{y}(t)$ or \mathbf{y} including EGC with coefficients \mathbf{u} is given as,

$$\mathbf{y}_{OFDM} = \mathbf{u}_{OFDM}^T \mathbf{x}_{OFDM} \quad (45)$$

A diagonal matrix \mathbf{u}_{OFDM} of dimensions $N \times N$ is considered. Matrix elements $\mathbf{u}_1^m(t)$, $\mathbf{u}_2^m(t)$, ..., $\mathbf{u}_n^m(t)$, ..., $\mathbf{u}_N^m(t)$ are on the diagonal. The column matrix \mathbf{x}_{OFDM} where the element n can be given by,

$$x_n(t + (p-1)\tau) = \frac{H_n^*}{|H_n|^2} r_n(t + (p-1)\tau) \quad (46)$$

2.3 Gradient Algorithm based BSS for DS-CDMA

Addition of interference has been recognized as one of the main limiting factors for the capacity of the most CDMA techniques. Basically this interference is generated from the other users in the system and from the external sources radiating in the same frequency band. Even if it is unlikely to control these types of interferences present in the environment efficiently, BSS algorithms can be developed to approach these scenarios.

Basic synchronous downlink DS-CDMA [18], [19] is considered. Channel impulse response for the path l of the channel tap of the multipath Rayleigh fading channel at time t is given by $A_l(t)$. Each tap is with L independent paths with exponentially decaying delay profiles.

$$\mathbf{A}(t) = \sum_{l=0}^{L-1} A_l(t) \quad (47)$$

The receive signal $r_j(t)$ at time t before despreading consisting K simultaneous users, can be expressed as in (48). Time t corresponds to the spreading code element j of each user.

$$r_j(t) = \sum_{k=1}^K \mathbf{A}(t) c_{k,j}(t) d_k(t) + \left(\frac{\sigma}{\sqrt{2}} n(t) \right) \quad (48)$$

Since slow fading is considered it can be assumed that for a given symbol frame path gain $\mathbf{A}(t) = \mathbf{A}$.

$$r_j(t) = \mathbf{A} \sum_{k=1}^K c_{k,j}(t) d_k(t) + \left(\frac{\sigma}{\sqrt{2}} n(t) \right) \quad (49)$$

where $c_{k,j}(t)$, $d_k(t)$ and $n(t)$ are spreading code element j of the user k at time t , transmit symbols of the user k at time t and normalized additive white Gaussian noise at time t respectively. σ is the standard deviation to the additive white Gaussian noise.

Signals at the receiver are sampled P times in small time shifts of τ within each spreading code element time duration where samples for $c_{k,j}(t)$ can be given as $r_j(t), r_j(t + \tau), \dots, r_j(t + (p-1)\tau), \dots, r_j(t + (P-1)\tau)$. They are equivalent to $x_1(t), x_2(t), \dots, x_f(t), \dots, x_F(t)$ in (1). Samples p of spreading code element sample $c_{k,j}(t)$, symbol $d_k(t)$ and additive white Gaussian noise are indicated by $c_{k,j}(t + (p-1)\tau)$, $d_k(t + (p-1)\tau)$ and $n(t + (p-1)\tau)$ correspondingly. Sample p of receive signal $\mathbf{r}_j(t)$ can be given as similar to (49),

$$r_j(t + (p-1)\tau) = \mathbf{A} \sum_{k=1}^K c_{k,j}(t + (p-1)\tau) \cdot d_k(t + (p-1)\tau) + \left(\frac{\sigma}{\sqrt{2}} n(t + (p-1)\tau) \right) \quad (50)$$

In a time duration of a spreading code element, for any sample $c_{k,j}(t + (p-1)\tau) = c_{k,j}(t)$ and $d_k(t + (p-1)\tau) = d_k(t)$.

$$r_j(t + (p-1)\tau) = \mathbf{A} \sum_{k=1}^K c_{k,j}(t) d_k(t) + \left(\frac{\sigma}{\sqrt{2}} n(t + (p-1)\tau) \right) \quad (51)$$

$\mathbf{r}_j(t)$ and $\mathbf{r}_j(t + \tau)$ are $Q \times Q$ square matrices containing these samples as elements and $(P-1) = Q^2$.

$$\mathbf{r}_j(t) = \begin{bmatrix} r_j(t) & \dots & \dots \\ \vdots & \ddots & \vdots \\ \dots & \dots & r_j(t + (P-2)\tau) \end{bmatrix} \quad (52)$$

$$\mathbf{r}_j(t + \tau) = \begin{bmatrix} r_j(t + \tau) & \dots & \dots \\ \vdots & \ddots & \vdots \\ \dots & \dots & r_j(t + (P-1)\tau) \end{bmatrix} \quad (53)$$

From (2) and (3),

$$\mathbf{C}(\tau) = \mathbf{E} \{ \mathbf{r}_j(t) \mathbf{r}_j^*(t + \tau) \} \quad (54)$$

$$\mathbf{R} = \mathbf{E} \{ \mathbf{r}_j(t) \mathbf{r}_j^*(t) \} \quad (55)$$

For the DS-CDMA systems coefficients for the algorithms can be introduced using (16) and (18). With mapping $\mathbf{u}_{1,1}^m(t)$ and $\mathbf{u}_{1,2}^m(t)$ to $\mathbf{h}_1^m(t)$ and $\mathbf{h}_2^m(t)$ respectively,

- *Common Coefficient 1*

$$\mathbf{h}_1^0(t) = \mathbf{h}_1(t) + \mu_{1,1} (\mathbf{I} - \mathbf{R} \mathbf{h}_1(t) \mathbf{h}_1^*(t)) \quad (56)$$

$$\cdot \mathbf{C} \mathbf{h}_1(t)$$

$$\mathbf{h}_1^m(t) = \frac{\mathbf{h}_1^{m-1}(t)}{\|\mathbf{h}_1^{m-1}(t)\|} \quad (57)$$

- *Common Coefficient 2*

$$\mathbf{h}_2^m(t) = \mathbf{h}_2(t) + \mu_{1,2} (\mathbf{I} - \mathbf{R} \mathbf{h}_2(t) \mathbf{h}_2^*(t)) \quad (58)$$

$$\cdot (\mathbf{C} + \mathbf{C}^*) \mathbf{h}_2(t)$$

$$\mathbf{h}_2^m(t) = \frac{\mathbf{h}_2^{m-1}(t)}{\|\mathbf{h}_2^{m-1}(t)\|} \quad (59)$$

For the iteration m of any of the solutions given for DS-CDMA is the same as (24) for the any of the solutions given by $\mathbf{h}_1^m(t)$ or $\mathbf{h}_2^m(t)$. But here also $\mathbf{h}_c^m(t)$ is different according to the scenario.

$$\mathbf{h}_c^m(t) = \frac{\mathbf{h}_c^{m-1}(t)}{\|\mathbf{h}_c^{m-1}(t)\|} \quad (60)$$

Refined receive signal similar to (4) is,

$$\mathbf{y}'_j(t) = \mathbf{h}_{c,j}^{m*}(t) \mathbf{r}_j(t) \quad (61)$$

Elements of matrix $\mathbf{y}'_j(t)$ can be defined as $y'_j(t), y'_j(t + \tau), \dots, y'_j(t + (p-1)\tau), \dots, y'_j(t + (P-1)\tau)$ similar to (49). Signal after EGC that is used for despreading can be expressed as,

$$\mathbf{y}_j(t) = \frac{1}{Q^2} \frac{\mathbf{A}^*}{|\mathbf{A}|^2} \sum_{p=1}^P y'_j(t + (p-1)\tau) \quad (62)$$

3 System Models

Two system models for OFDM and DS-CDMA are separately considered under the same conditions. A downlink frequency-selective slow fading Rayleigh channel is used as the air interface. It is assumed that perfect path gain values are available at the receivers and transmit receiver setups are properly synchronized under all the conditions. EGC, one of the most stable combining technique is used to treat CSIs.

3.1 OFDM System Model

Elementary system model used for discrete time base band simulations is given in Figure 1. The single transmit and single receive antenna setup is equipped with an OFDM transmitter and a receiver [17], [18]. Receiver is supplemented with lesser complex iterative BSS algorithms with multiple sampling for each receive symbol on each subcarrier. Same system model without multiple sampling is used in order to test and verify the results of standard OFDM system [17], [18].

3.2 CDMA System Model

The DS-CDMA discrete time base band simulation system model in Figure 2 is consist of a transmitter [19] [18] which can handle K users using Walsh-Hadamard spreading sequences [19]. At the receiver, multiple samples for each receive spread code element are taken. Then iterative lesser complex Gradient principles based BSS algorithms followed by EGC are employed. Same system model with no multiple sampling mechanism for receive spread code elements is used in order to test and verify the results comparing with a standard downlink synchronous DS-CDMA system [19], [18].

4 System Parameters and Simulation Results

System parameters and simulation results for the both categories of techniques are separately presented. Simulations are carried out for non optimized forgetting factor with value -0.01. Each channel tap is modeled with 4 independent paths and it is assumed that there is no variation of the signal within symbol duration due to any other reason. Since the system is operated under slow fading conditions the assumption becomes much stronger.

4.1 OFDM Systems

Standard or basic 64, 32 and 16 subcarrier OFDM transmitter receiver arrangements with a binary information bit generator and binary phase shift keying (BPSK) symbol mapping are used for the simulations. After interleaving,

symbols are serial to parallel converted among subcarriers and sent through the slow Rayleigh fading channel. Multiple signal samples are taken from each receive symbol on every subcarrier for the purpose of using GA based BSS schemes. By considering the characteristics of the channel [20] and time correlation properties of the binary wave forms [16], samples are taken only within the first 20% of time duration of an information symbol. Systems with the BSS schemes are configured to be operated a number of iterations.

In the case of first set of simulations, variable number of subcarriers for the BSS scheme is considered. Performance results for 16, 32 and 64 subcarriers are obtained for this classification with processing matrix size 4 (5 receive signal samples) for each of the receive symbol on every subcarrier. Rest of the parameters and conditions of the model are maintained as the same. Outcome of the operations of the systems namely the OFDM system with the BSS algorithms and the standard OFDM system is presented in Figures 3 and 4. The results of the schemes 1 (coefficient $\mathbf{u}_{1,1,n}^m(t)$ in (35)) and 2 (coefficient $\mathbf{u}_{1,2,n}^m(t)$ in (37)), worked out for 16, 32 and 64 subcarriers are given by Figure 3 - (a) and (b) separately. In this case the algorithms based OFDM systems are competent of outperforming the corresponding standard OFDM systems. It is important to notice that the performance of the algorithms are better when the signal to noise ratio (SNR) is higher and performance of the standard systems are comparatively better for the lower SNR values. Similarly the results of the schemes 3 (coefficient $\mathbf{u}_{2,1,n}^m(t)$ in (39)) and 4 (coefficient $\mathbf{u}_{2,2,n}^m(t)$ in (41)) worked out for 16, 32 and 64 subcarriers are given by Figure 4 - (a) and (b) respectively. In these cases also, the algorithms based OFDM systems are capable of outperforming the corresponding standard OFDM systems in respective subcarriers scenarios. In all occasions, performance is better when the number of subcarriers are increased.

Corroborative simulations conducted using the explained OFDM substructure with the BSS algorithm with different processing matrix sizes and the standard OFDM system are shown in Figure 5 and 6. Other parameters and conditions are maintained as the same. Performance is scrutinized for the BSS schemes 1 (coefficient $\mathbf{u}_{1,1,n}^m(t)$ in (35)) and 2 (coefficient $\mathbf{u}_{1,2,n}^m(t)$ in (37)) carried out for processing matrix sizes 4 and 9 and presented in Figure 5 - (a) and (b) respectively. Outcome of the both algorithms with matrix size 9 (10 samples) is shown in Figure 5 - (c) where the simulation curves of the two schemes fall in the vicinity of each other for higher SNR values while showing a clear difference for lower SNR values. Better bit error rates are demonstrated by the curves taken for a higher processing matrix size. Hence it could be resolved that a constructive contribution is done by a larger processing matrix for the process of refinery of corrupted symbols under these parameters. Same way, outcomes of the simulations carried out for the BSS schemes 3 (coefficient $\mathbf{u}_{2,1,n}^m(t)$ in (39))

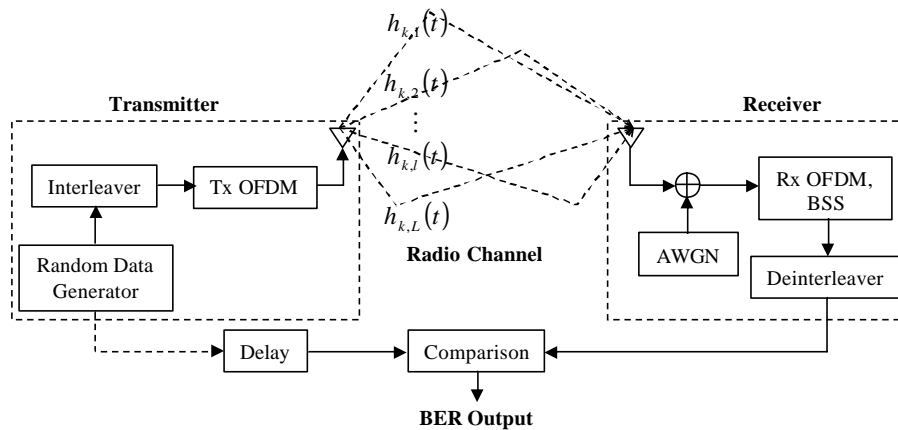


Fig. 1. Block diagram of the lowpass equivalent OFDM system model

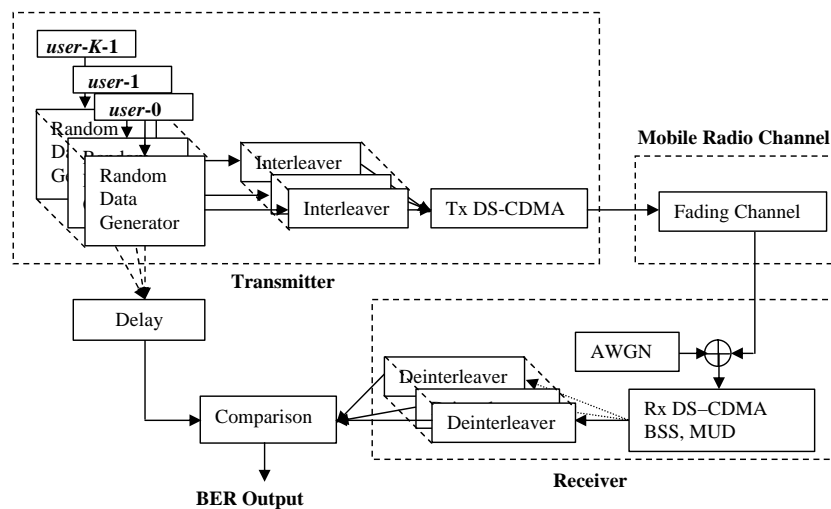


Fig. 2. Block diagram of the lowpass equivalent DS-CDMA system model

and 4 (coefficient $\mathbf{u}_{2,2,n}^m(t)$ in (41)) with processing matrix sizes 4 and 9 and presented in Figure 6 - (a) and (b) respectively. Results of the both algorithms with matrix size 9 is shown in 6 - (c) where the simulation curves of the two schemes fall in the vicinity of each other. Better bit error rates are demonstrated by the curves of taken for a higher processing matrix sizes. Hence it could be observed that a constructive contribution is done by a larger processing matrices for the process of detection of corrupted information symbols under these parameters.

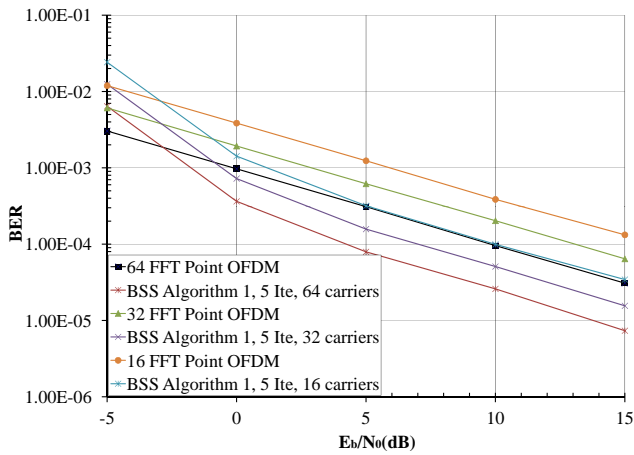
4.2 DS-CDMA Systems

Systems consisting 16-users with a 16 Walsh-Hadamard code matrices [19] are considered for simulations. Binary information bit streams of each user are converted to binary phase shift keying (BPSK) symbols, interleaved and transmitted through slow fading channel. Multiple signal samples are obtained corresponding to each of the receive spread code element for the purpose of using the Gradient Algorithm based BSS schemes. Considering the properties of the channel [20] and time correlation properties of the binary wave forms [16] it is decided to take samples only

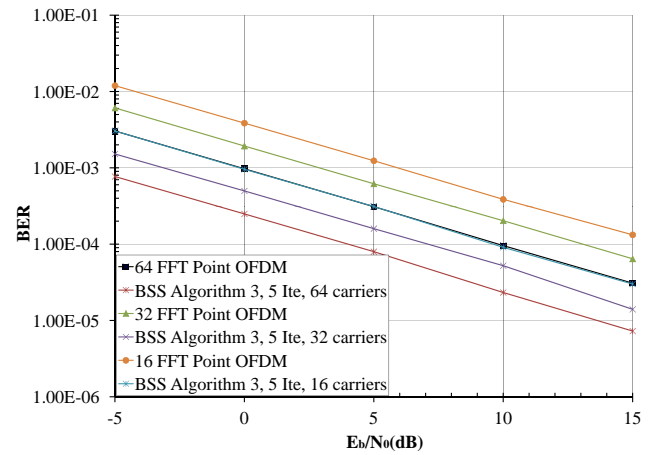
within the first 20% of time duration of a spread sequence element. Systems with the BSS schemes are configured to be operated for number of iterations.

Performance of the DS-CDMA systems viz. system with two BSS algorithms and standard DS-CDMA system for different number of users are shown in Figure 7. All the other parameters and conditions are maintained as the same. The results obtained with the both BSS schemes carried out for 2, 4, 8 and 16 users with 5 iterations are presented in Figure 7 - (a) and (b) respectively. Curves of the 2, 4, 8 and 16 users scenarios fall vicinity of each other as usual. Each receive spread code element is sampled 5 times at the receiver creating processing matrix size 4. Here the standard DS-CDMA system is outperformed by the these algorithms.

Similarly another set of simulation results are obtained with different processing matrix sizes for the BSS scheme and each receive spread code element comparing with the standard DS-CDMA system as indicate by Figure 8. In this development all these algorithms are capable of outperforming the standard DS-CDMA system. Figure 8 -



(a)



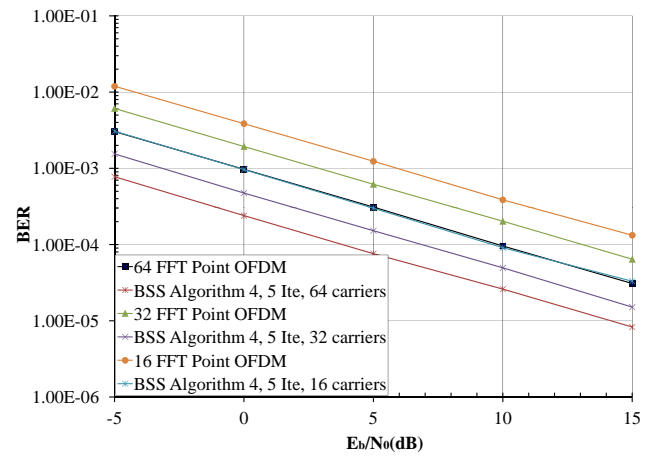
(b)

Fig. 3. OFDM systems with BSS, EGC and Matrix Size 4 : (a) algorithm 1 and (b) algorithm 2

(a) and (b) are used for algorithms 1 and 2 respectively with the processing matrix sizes 4 and 9, while the performance of both algorithms with the processing matrix size 9 is given by Figure 8 - (c). Number of iterations are confined to 5 in all cases. It could be noted that the process of refinery of corrupted signals is contributed positively by taking a higher number of samples or larger matrix sizes under these parameters.

5 Conclusion

A solutions developed attempting to achieve a better signal recovery in a observe mixture in a free space communication channel of OFDM and DS-CDMA transmissions based on gradient algorithms and BSS principles were considered. In the case of OFDM, performance was evaluated in recovery of information symbols mitigating the deteriorative effects under the categories of variable subcarriers for the systems and matrix sizes for receive symbols. In the case of DS-CDMA, performance was evaluated under the categories of variable number of users for the systems and matrix sizes for receive symbols. It could be observed that the signal detection was better performed



(a)

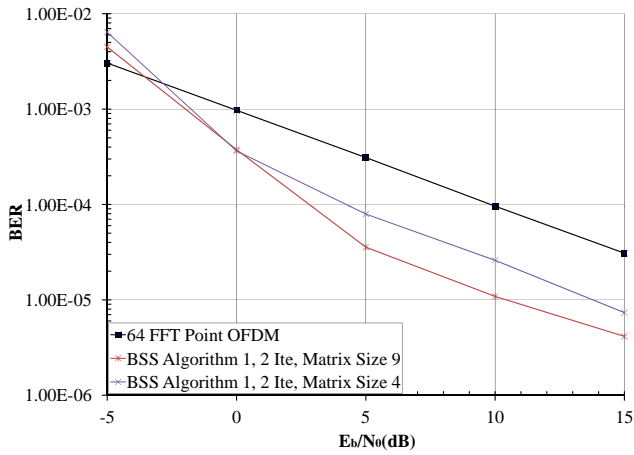
Fig. 4. OFDM systems with BSS, EGC and Matrix Size 4 : (a) algorithm 3 and (b) algorithm 4

by the algorithms when the size of the processing matrix was higher. Though it is not quantified with in this study, the algorithms could be introduced as low computational complexity, matrices based processing schemes. Further studies on the algorithms can be done with optimizing the forgetting factor and covering Doppler effect before they are being tested in a real atmosphere.

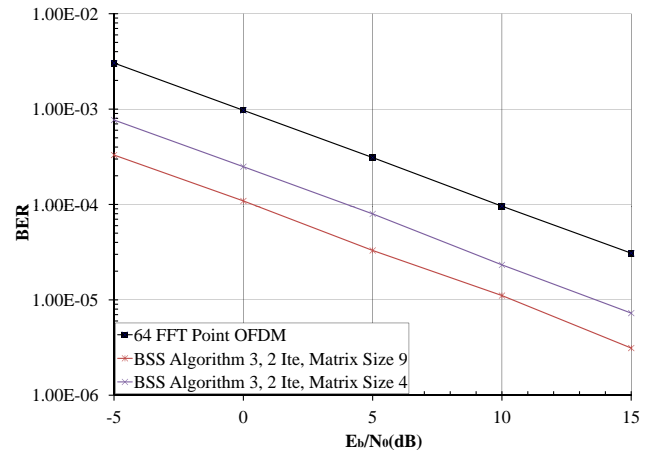
REFERENCES

- [1] J. -F. Cardoso, "Blind Signal Separation: Statistical Principles," *Proceedings of the IEEE*, vol. 86(10), pp. 2009-2025, October 1998.
- [2] M. E. Sahin, I. Guvenc, and H. Arslan, "Uplink User Signal Separation for OFDMA-Based Cognitive Radios," *EURASIP Journal on Advances in Signal Processing*, Hindawi Publishing Corporation, vol. 2010, Article ID 502369.
- [3] X-L. Li, and T. Adali, "Blind Separation of Noncircular Correlated Sources using Gaussian Entropy Rate," *IEEE Transactions on Signal Processing*, vol. 59, no. 6, pp. 2969-2975, 2011.
- [4] F. Abrard, and Y. Deville, "A Timefrequency Blind Signal Separation Method Applicable to Underdetermined Mixtures of Dependent Sources," *Elsevier Journal on Signal Processing*, Elsevier B. V., vol. 85, pp. 13891403, 2005.
- [5] R. L. Adler, J. -P. Dedieu, J. Y. Margulies, M. Martens, and M. Shub, "Newtons method on Riemannian manifolds and a geometric model for the human spine," *IMA Journal of Numerical Analysis*, vol. 22(3), pp. 359-390, July 2002

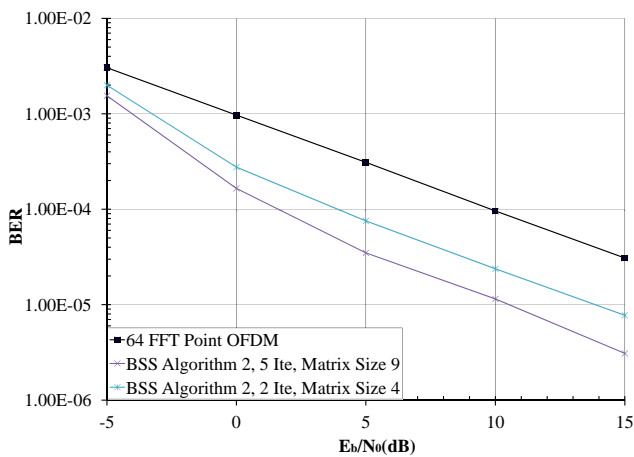
- [6] A. K. Barros, R. Vigário, V. Jousmäki, and N. Ohnishi, "Extraction of Event-related Signals from Multichannel Bioelectrical Measurements," *IEEE Transaction on Biomedical Engineering*, vol. 47, no. 5, pp. 583-588, May 2000.
- [7] N. Mammone, F. La Foresta, and F. C. Morabito, "Automatic Artifact Rejection From Multichannel Scalp EEG by Wavelet ICA," *IEEE Sensors Journal*, vol. 12, no. 3, pp. 533-542, March 2012.
- [8] M. E. Waheed, "Blind Signal Separation using an Adaptive Weibull Distribution," *International Journal of Physical Sciences*, vol. 4(5), pp. 265-270, May 2009.
- [9] S. Boyd, and L. Vandenberghe, *Convex Optimization*. Cambridge University Press, 2004.
- [10] H. Nguyen, and R. Zheng, "Binary Independent Component Analysis With or Mixtures," *IEEE Sensors Journal*, vol. 59, no. 7, pp. 3168-3181, July 2011.
- [11] J. Moragues, L. Vergara, and J. Gosálbez, "Generalized Matched Subspace Filter for Nonindependent Noise Based on ICA," *IEEE Transactions on Signal Processing*, vol. 59, no. 7, pp. 3430-3434, July 2011.
- [12] F. Nesta, P. Svaizer, and M. Omologo, "Convolutive BSS of Short Mixtures by ICA Recursively Regularized Across Frequencies," *IEEE Transactions on Audio, Speech, and Language Processing*, vol. 19, no. 3, pp. 624-639, March 2011.
- [13] J. Gao, X. Zhu, H. Lin, and A. K. Nandi, "Independent Component Analysis Based Semi-blind I/Q Imbalance Compensation for MIMO OFDM Systems," *IEEE Transactions on Wireless Communications*, vol. 9, no. 3, pp. 914-920, March 2010.
- [14] A. Belouchrani, K. Abed-Meraim, J.-F. Cardoso, and E. Moulines, "A Blind Source Separation Technique using Second-Order Statistics," *IEEE Transactions on Signal Processing*, vol. 45, no. 2, pp. 434-444, February 1997.
- [15] L. Parra, and P. Sajda, "Blind Source Separation via Generalized Eigenvalue Decomposition," *The Journal of Machine Learning Research*, vol. 4, pp. 1261-1269, December 2003.
- [16] S. Haykin, *Communication Systems*. John Wiley & Sons, Inc. 4th Edition, 2001.
- [17] C. K. Sung, and I. Lee, "Multiuser Bit-Interleaved Coded OFDM with Limited Feedback Information," *IEEE Vehicular Technology Conference*, Dallas, Texas, USA, September 2005.
- [18] L. Hanzo, L.-L. Yang, E.-L. Kuan, and K. Yen, *Single- and Multi-Carrier DSCDMA: Multi-User Detection, Space-Time Spreading, Synchronisation, Networking and Standards*. John Wiley & Sons, Inc. 2003.
- [19] S. Verdú, *Multiuser Detection*. Cambridge University Press, Cambridge, U.K. 1998.
- [20] J. G. Proakis, *Digital Communications*. McGraw-Hill, Inc. 4th Edition, 2001.



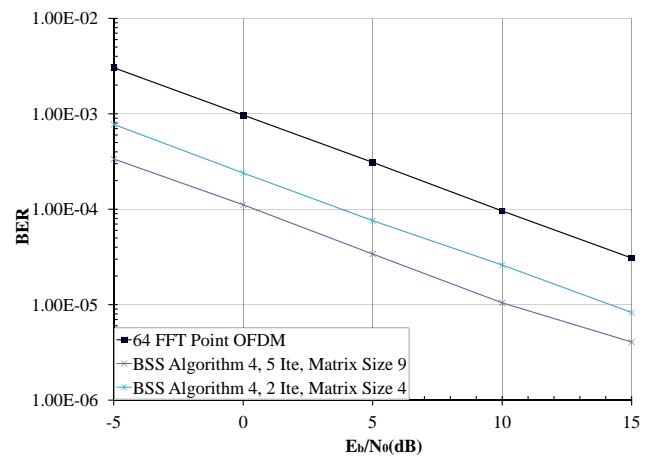
(a)



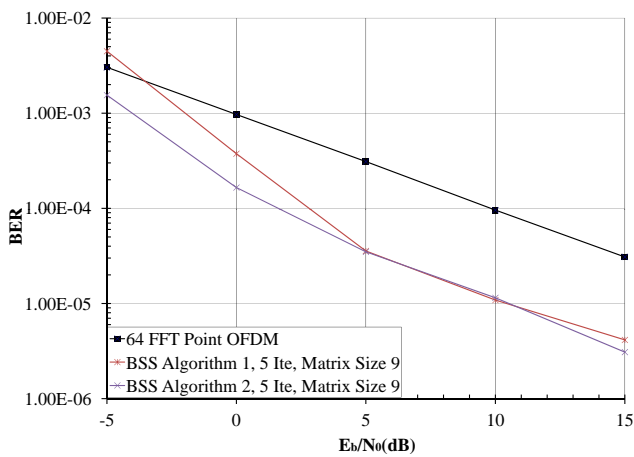
(a)



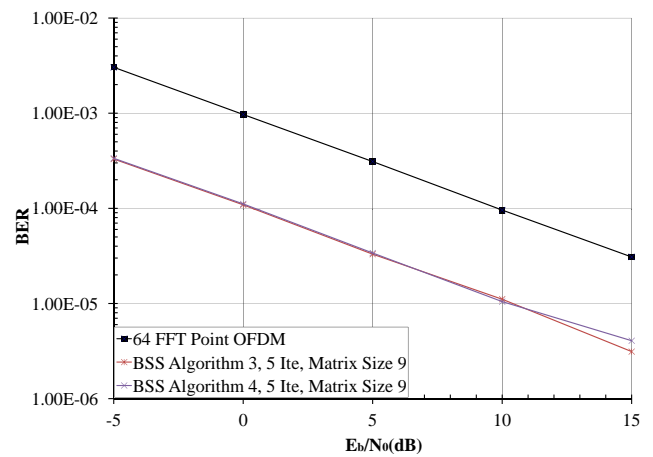
(b)



(b)



(c)



(c)

Fig. 5. OFDM systems with BSS and EGC : (a) algorithm 1, (b) algorithm 2 and (c) two algorithms with matrix size 9

Fig. 6. OFDM systems with BSS and EGC : (a) algorithm 3, (b) algorithm 4 and (c) two algorithms with matrix size 9

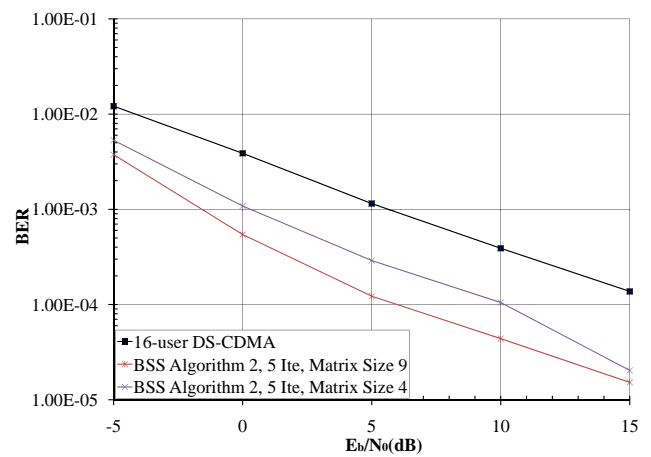
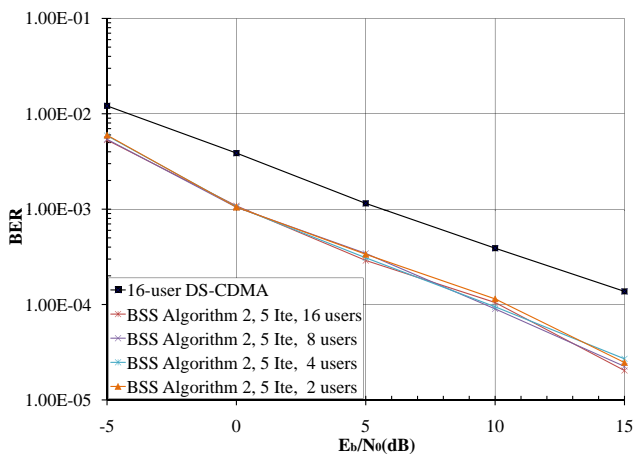
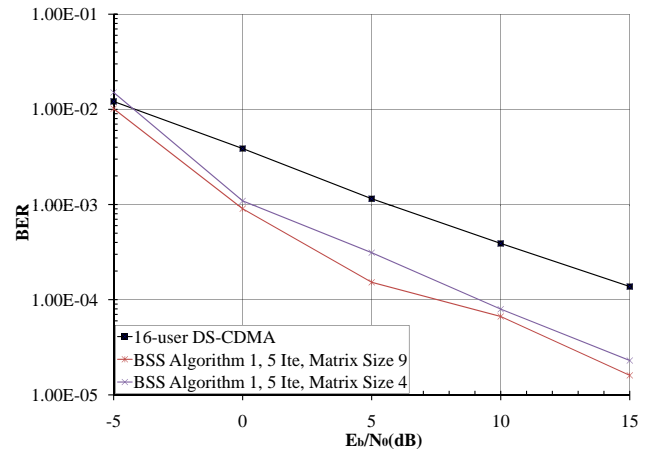
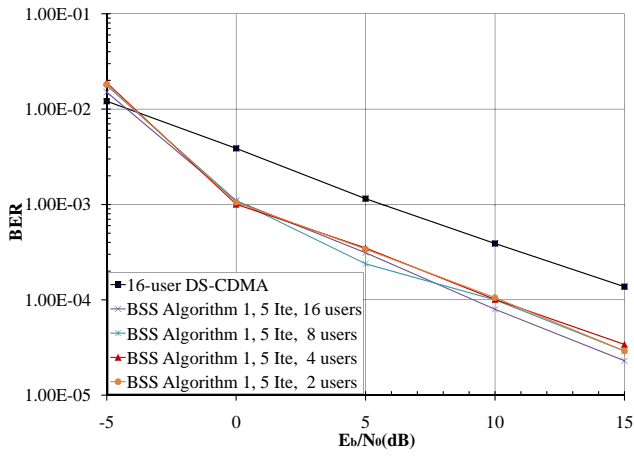


Fig. 7. 32-user DS-CDMA systems with BSS and EGC : (a) algorithm 1 and (b) algorithm 2

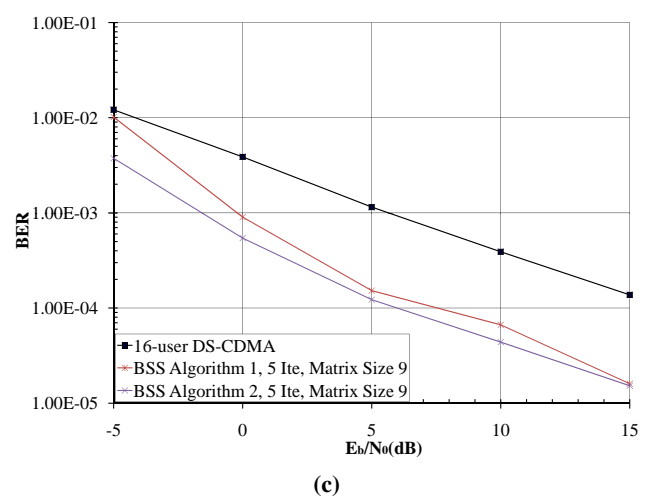


Fig. 8. 32-user DS-CDMA systems with BSS and EGC : (a) algorithm 1, (b) algorithm 2 and (c) two algorithms with matrix size 9